

3.2.2. AEROSOL MEASUREMENTS AT MLO DURING MLOPEX

Introduction

The routine aerosol monitoring program was initiated at MLO in 1974 with the installation of instrumentation for the continuous measurements of CN concentration and aerosol scattering extinction coefficient (σ_{sp}), although apparently the earliest aerosol measurements were made by Nakaya *et al.* [1957]. A brief history of MLO aerosol measurements was given by Bodhaine [1983].

The Mauna Loa Observatory Photochemistry Experiment (MLOPEX) was a multi-agency cooperative experiment designed to study the chemistry of the free troposphere near 3.4-km altitude. The experiment consisted of four intensives that were designed to obtain data representative of four different seasons at MLO. The periods chosen were September 16-October 23, 1991; January 15-February 15, 1992; April 12-May 15, 1992; and July 15-August 14, 1992. An important part of this experiment was to investigate the diurnal cycles of the parameters measured, both the effects of the upslope-downslope windflow, and the diurnal photochemical cycles in free tropospheric air. All dates and times are presented here as Julian day-of-year (DOY) and Hawaii Standard Time (HST). For comparison with Universal Time (UT), UT = HST + 10 hours at MLO.

Instrumentation

CN measurements were initiated in 1974 using a G.E. automatic CN counter (1974-1989) and a TSI 3760 CN counter (1989-present). A Pollak CN counter [Metnieks and Pollak, 1959] has been operated daily since 1974 to provide comparison points for the automatic CN counters. Aerosol scattering extinction coefficient (σ_{sp}) measurements were initiated in 1974 using a four-wavelength nephelometer similar to the design of Ahlquist and Charlson [1969]. Aerosol absorption (σ_{ap}) has been measured at MLO since 1990 using an aethalometer [Hansen *et al.*, 1982]. The instrument and data for 1990-1991 were described by Bodhaine *et al.* [1992]. The SO₂ data shown here were provided by Gerd Hübler (personal communication, 1994).

Data Analysis

Diurnal cycles. Data from intensives 3 and 4 were used to study the character of the diurnal cycle at MLO. **Figure 3.21** shows means by hour of the day for the entire periods of intensives 3 and 4. The primary data set used to form these means was the hourly data produced by the MLO data acquisition system. An hourly data point was deemed acceptable for inclusion in the mean if the 450-, 550-, and 700-nm nephelometer data were all present and if no local pollution was detected during that hour. Next, the Ångström exponent (α) was calculated from the σ_{sp} data. Finally, if CN, wind direction (WD), or wind speed (WS) data were present for that hour, they were included in their means for that hour of the day. Thus the tallies of

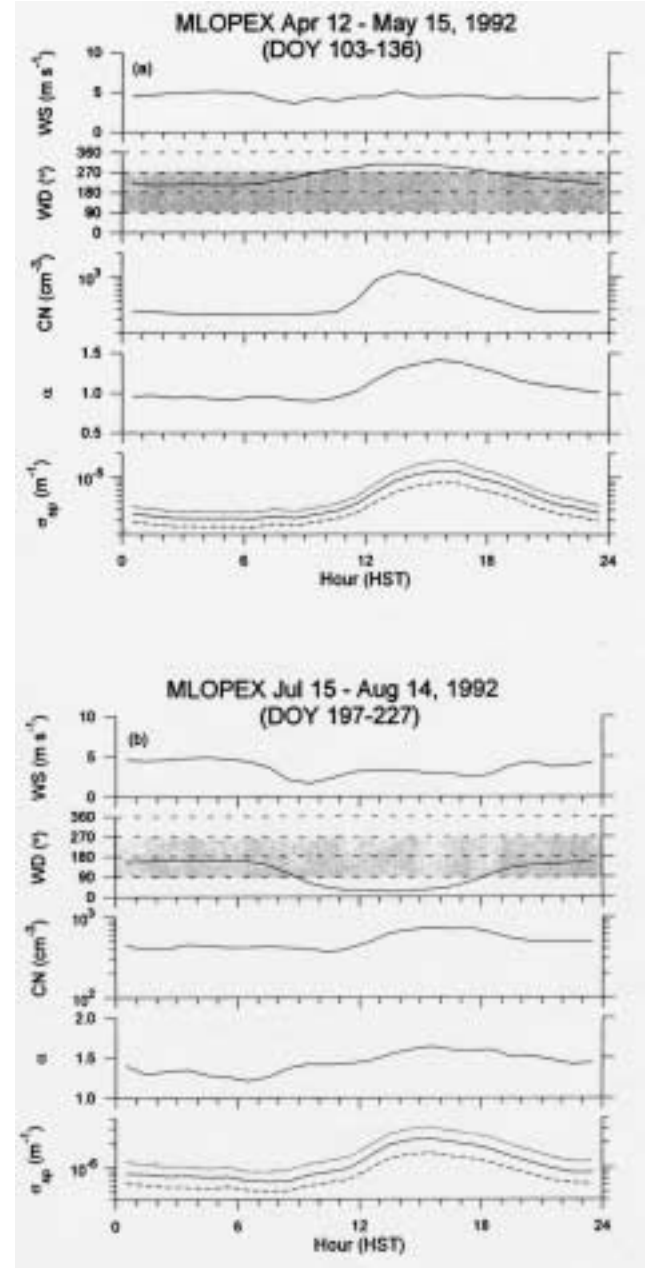


Fig. 3.21. Data for MLOPEX (a) intensive 3 and (b) intensive 4. Means by hour are shown for wind speed (WS); wind direction (WD); CN concentration; α ; and σ_{sp} for 450 (dotted), 550 (solid), and 700 nm (dashed). α values were calculated using equation (1). The shaded areas on the WD graphs denote winds with a southerly (downslope) component. Hour of the day is shown as HST.

σ_{sp} , CN, WD, and WS, could all be different for a given hour. However, this procedure was necessary to avoid problems caused by missing data when several data sets are merged.

Referring to Figure 3.21a, the average diurnal range in CN concentration was about 300-1000 cm^{-3} between night and day, with the beginning of background sampling conditions at about 2100 HST and the onset of the upslope wind at about 1000 HST. The σ_{sp} data show somewhat narrower background sampling conditions between about 0200 and 0800. Historically, 0000-0800 was the time interval chosen to sample background values of σ_{sp} at MLO [Bodhaine, 1978]. The WD data in Figure 3.21a show clearly that WD changes from northerly to southerly at about 1800, and back to northerly at about 0900. Clearly, a time lag exists between when WD changes and when stable sampling conditions exist at the site. WS averaged about 5 m s^{-1} during both night and day.

The α data in Figure 3.21a show that the particle size tended to be larger during downslope conditions than during upslope conditions during this intensive. Particle sizes are generally larger at this time of year because of Asian dust transport. The interpretation of α data has been discussed by Bodhaine and DeLuise [1985]; however, qualitatively speaking, larger α 's imply smaller particles and vice versa.

Figure 3.21b shows a similar presentation of the average MLO diurnal cycle during intensive 4. Aerosol scattering extinction coefficient values are about a factor of five lower than in intensive 3. A diurnal cycle of σ_{sp} is apparent with background conditions occurring during about 2200-0800. WD shows an upslope-downslope effect with a change to southerlies at 1800 and the onset of the upslope at 0800. In the summer (Figure 3.21b) the winds had an easterly component whereas in the spring (Figure 3.21a) the winds had a westerly component. Also, note that the winds were weaker during the upslope-downslope transition periods.

A classic example of an upslope-downslope event with clean background conditions during downslope flow, is shown in Figure 3.22 for DOY 118-119 (April 27-28) 1992. Here the CN concentration shows clean conditions from 1700 on DOY 118 to 1000 on DOY 119, and WD is clearly in the southerly band during that time. The σ_{sp} data are interesting because they apparently settle to background values by about 2000 on DOY 118, but assume a new, lower value during about 0800-1100 on DOY 119 before the upslope event appears. This behavior may be explained by a decrease in aerosol concentration at about 0800 on DOY 119 (possibly by a few large dust particles), which gave an obvious decrease in σ_{sp} and an increase in α , but a negligible effect on the CN concentration. Note the fairly high WS on these two days. The SO_2 data superimposed here in Figure 3.22 follow the CN data quite closely, indicating an island source for SO_2 . These local sources of SO_2 could be either anthropogenic (e.g., fuel combustion) or natural (e.g., fuming from Kilauea caldera). The black carbon (BC) data in Figure 3.22 show a diurnal cycle that follows the CN and SO_2 data quite closely, suggesting similar sources. Since BC can be produced locally by both natural and anthropogenic

sources, it can be a good indicator of a local pollution event.

Asian desert dust event. Examples of Asian dust events are shown in Figure 3.23. Episodes of closely-spaced three-wavelength σ_{sp} data (low values of α) strongly suggest a relatively larger aerosol size, most likely Asian dust [Bodhaine *et al.*, 1981]. The σ_{sp} data in Figure 3.23, at the beginning of DOY 126, show the end of a downslope event dominated by large particles at about 0800 and smaller upslope particles at about 1200. The large particle peak was about $2 \times 10^{-5} \text{ m}^{-1}$ with an α near 0. By about 0000 on DOY 127 the data show a small-particle downslope regime, illustrating the patchy nature of the Asian dust. Large particles dominated the upslope-downslope cycle that began at about 0800 on DOY 127 and continued through about 1000 on DOY 128. Similar effects occurred over the next several days and the Asian dust was gone by about DOY 134.

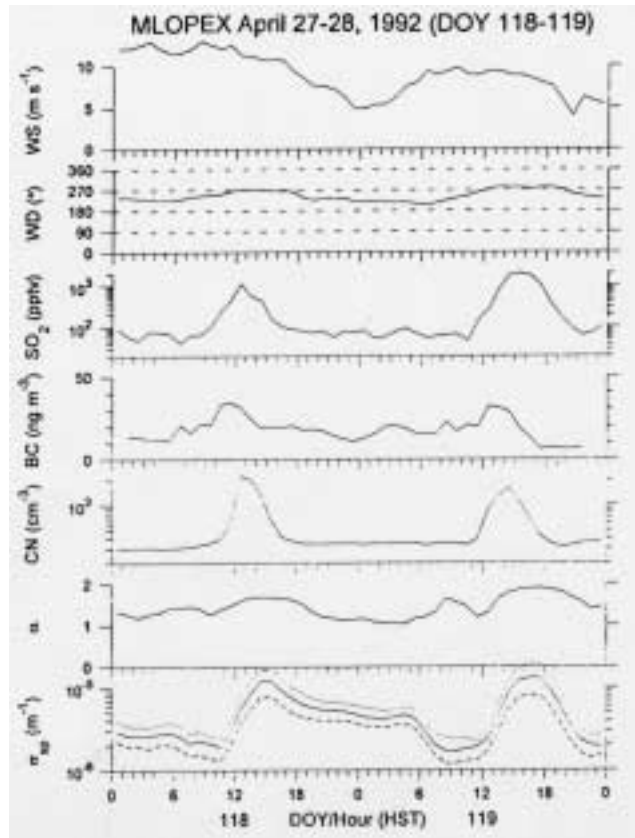


Fig. 3.22. Hourly values of wind speed (WS); wind direction (WD); SO_2 concentration; BC concentration; CN concentration; α ; and σ_{sp} for 450 (dotted), 550 (solid), and 700 nm (dashed), on DOY 118-119, 1992. α values were calculated using equation (1). The shaded area on the WD graph denotes winds with a southerly (downslope) component. Hour of the day is shown as HST.

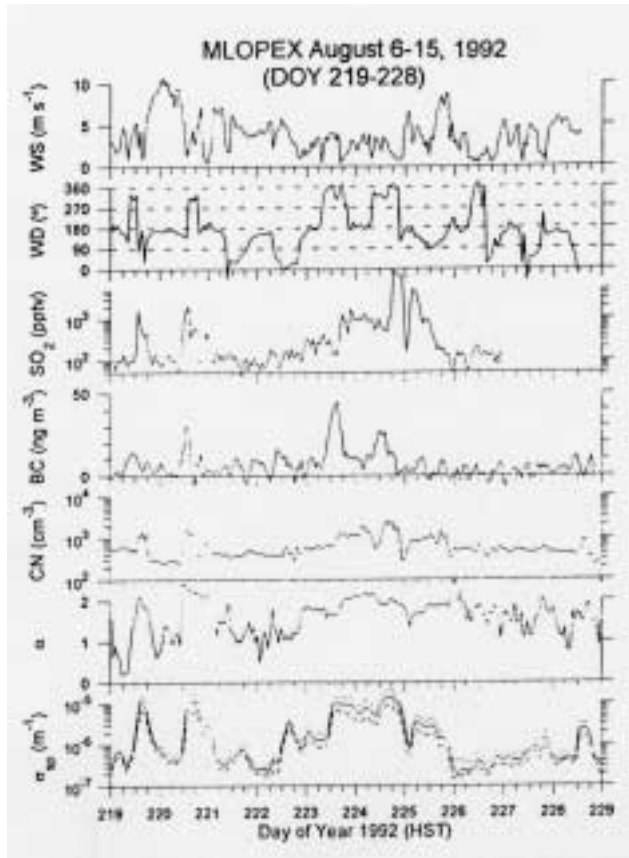


Fig. 3.23. Hourly values of wind speed (WS); wind direction (WD); SO_2 concentration; BC concentration; CN concentration; α ; and σ_{sp} for 450 (dotted), 550 (solid), and 700 nm (dashed), on DOY 126-135, 1992, during which an Asian desert dust event occurred. α values were calculated using equation (1). A 3-hour running mean was applied to the BC data. The shaded area on the WD graph denotes winds with a southerly (downslope) component. Hour of the day is shown as HST.

At about 1000 on DOY 128, 129, and 130 three obvious small-particle upslope events broke through the Asian dust cloud. Note the clean downslope event on DOY 135 that gave σ_{sp} values of about 5×10^{-7} and CN concentrations of about 300 cm^{-3} , even though WD did not indicate strong downslope conditions. The multi-wavelength σ_{sp} data clearly identify the presence of large Asian dust particles as opposed to smaller background-tropospheric or locally-produced particles. Note that Asian dust can dominate the aerosol measurements during upslope as well as downslope flow.

The SO_2 data for this period appear to correlate best with the CN data, and the α data show that SO_2 events tend to be correlated with small-particle events. Of particular interest is the fact that SO_2 events occur during the Asian dust events, raising the possibility that SO_2 may be transported from Asia. The BC data shown in Figure 3.23 tend to follow the σ_{sp} data during the beginning of the record and the CN and SO_2 data during the latter part

of the record. This suggests that the BC may have been transported over long distances when it is associated with the desert dust as determined from the σ_{sp} data [Bodhaine *et al.*, 1992].

Mixed regime. Data for DOY 219-228 are presented in Figure 3.24. This 10-day period was chosen to illustrate the difficulty of just classifying MLO data as upslope or downslope. This was a period of generally light and somewhat uncertain winds (with the exception of DOY 220). The particle size distribution, as suggested by the σ_{sp} and α data, was dominated by small particles during both upslope and downslope conditions throughout the entire period. The α data here tend to be somewhat noisier than those during the Asian dust period because the σ_{sp} data are much lower. The cleanest background conditions exhibit σ_{sp} values of about $2 \times 10^{-7} \text{ m}^{-1}$ and CN concentrations of about 300 cm^{-3} on DOY 222 and during the clean period of 226-227.

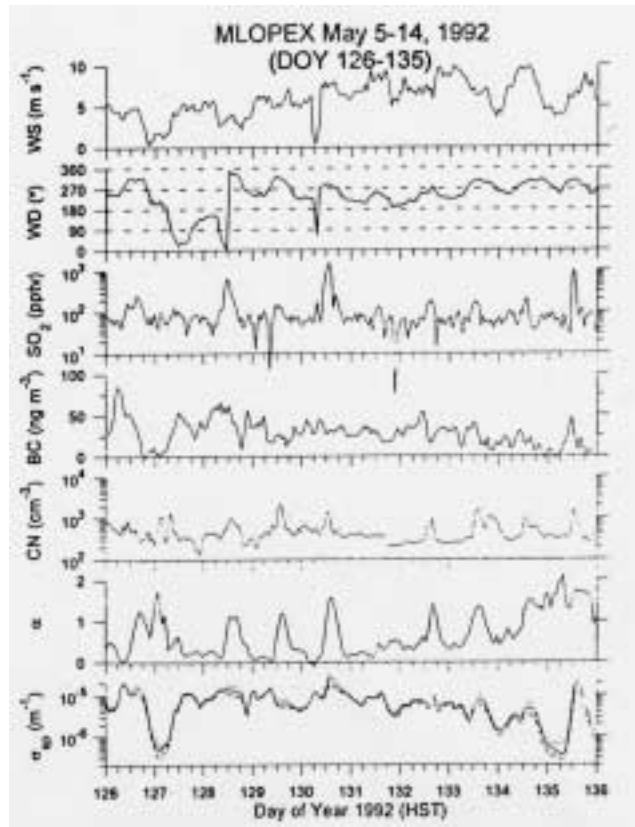


Fig. 3.24. Hourly values of wind speed (WS); wind direction (WD); SO_2 concentration; BC concentration; CN concentration; α ; and σ_{sp} for 450 (dotted), 550 (solid), and 700 nm (dashed), on DOY 219-228, 1992, during which rather uncertain conditions existed. α values were calculated using equation (1). A 3-hour running mean was applied to the BC data. The shaded area on the WD graph denotes winds with a southerly (downslope) component. Hour of the day is shown as HST.

The upslope event at about 1200 on DOY 219 is quite obvious in the σ_{sp} , α , CN, and SO_2 data. However, it is not so easy to predict based on WD and WS data. The next upslope event at about 1200 on DOY 220 again shows up clearly in all data records and does have a northerly WD. The secondary peak at about 2300 on DOY 220 appears during southerly winds but seems to be associated with a minimum in WS. Then a strong downslope at 0200 on DOY 221 gave clean conditions before the next upslope event in σ_{sp} at about 1200 on DOY 221.

The downslope event at about 1800 on DOY 221 produced very clean background conditions in both σ_{sp} and CN data, followed by classic upslope wind flow at about 0800 on DOY 222. The secondary event in σ_{sp} (but not in CN) at about 0000 on DOY 223 is unexpected and not easily explained on the basis of these data alone. Likewise, the obvious upslope events at about 1200 on DOY's 223 and 224 are expected, but the polluted values during 0000-1200 on DOY 224 or the peak beginning at about 0200 on DOY 225 are not expected. A clean period begins at about 0000 on DOY 226 and continues until the upslope event begins at about 0800 on DOY 228. Note, however, the slight upslope event at about 0800 on DOY 226 and the spurious event at about 2000 on DOY 227, apparently associated with light winds.

Referring to the SO_2 data in Figure 3.24, it is possible to explain the unexpected features discussed previously. These data show peaks of about 2 ppbv that coincide with the upslope events at about 1200 on DOY 219 and 220. However, a peak during downslope conditions at about 2300 on DOY 220 coincides with those in CN and σ_{sp} . SO_2 events at 0000 on DOY 223, 0000 on DOY 224, 1800

on DOY 224, and 0200 on DOY 225 all occur during downslope conditions and are most likely caused by venting from the Mauna Loa caldera.

The BC data shown in Figure 3.24 tend to follow upslope events, although not always. The three largest events in the BC data coincide with upslope events; however, the volcanic events discussed previously show low BC concentrations. Note the extremely low BC concentrations during DOY 226-227, probably representative of clean background tropospheric conditions.

Data screening. Clearly it would be difficult to design a computer algorithm for routinely screening data that could cope with the data shown in Figures 3.23 and 3.24. Historically, MLO aerosol data were screened on the basis of time of day and WD. The time window 1000-1800 UT for accepting background σ_{sp} data was used by *Bodhaine* [1978], based on 3 years of nephelometer data. This time window allows for the slow time response of the nephelometer. Wind criteria for accepting MLO aerosol data require WD with a southerly component ($90^\circ < WD < 270^\circ$) and $WS > 0.5 \text{ m s}^{-1}$ [*Bodhaine et al.*, 1980]. Currently, routine MLO aerosol data editing also includes the manual identification of suspicious hours that may have been influenced by some unknown short-term local activity. These hours are labeled with "P" flags [*Massey et al.*, 1987]. It is apparent from the previous examples that MLO data should be edited on a day-by-day basis, using as many different data sets as possible, including SO_2 and BC concentration. Continuous SO_2 measurements at MLO would be extremely desirable.